IEEE 802.15.4 Air-Ground UAV Communications in Smart Farming Scenarios

Manlio Bacco, Andrea Berton, Alberto Gotta, Luca Caviglione

***Abstract*—Smart farming is one of the most promising applications showing the benefits of using unmanned aerial vehicles (UAVs). Thus, precision agriculture in rural areas may largely benefit from low-cost and easy-to-deploy vehicles able to exchange data with ground sensors for monitoring and controlling automated cultivations. In this letter, we describe, both analytically and empirically, a real testbed implementing IEEE 802.15.4-based communications between an UAV and fixed ground sensors. In our scenario, we found that aerial mobility limits the actual IEEE 802.15.4 transmission range among the UAV and the ground nodes to approximately 1/3 of the nominal one. We also provide considerations to design the deployment of sensors in precision agriculture scenarios.**

I. Introduction

Unmanned Aerial Vehicles (UAVs) are increasingly used in several scenarios, including goods delivery, environmental monitoring, public protection, and disaster relief [1]. Smart agriculture and smart farming are ones of the most promising scenarios where UAVs can leverage their power. As possible examples, they can undertake remote sensing campaigns, spray chemicals, apply variable rate treatments, create vegetation indexes, and gather data from a variety of sensors deployed in the field [2][3]. To this aim, an UAV should be able to communicate with a ground station, IoT nodes, or wireless sensors [3]. Owing to its cost-effectiveness, a large availability on the market, and a low-power footprint, IEEE 802.15.4 should be preferred over IEEE 802.11 in terms of power efficiency [4] and over 3G/4G mobile networks, which may provide sporadic coverage in rural areas [5]. Moreover, precision agriculture applications often require short-range communications, thus making IEEE 802.15.4-based systems a convenient choice.

To effectively exploit UAVs for smart farming, the performances of the short-range wireless link must be carefully addressed and this letter focuses on its characterization at packet level. This allows to engineer the protocol stack, optimize mission parameters, or pursue energy efficiency. The IEEE 802.15.4 standard has been widely investigated in both outdoor and indoor scenarios. However, only few works explicitly consider the impact of aerial mobility, e.g., in terms of speed of the UAV, orientation of antennas, or signal strength [6], [7]. An important contribution on the behavior of IEEE 802.15.4 can be found in reference [8], where the authors investigate several metrics, including the packet loss. Unfortunately, the study is limited to links used by road vehicles to exchange data peer-to-peer or with a road infrastructure. The framework presented in [9] addresses the design of a winged vehicle, using IEEE 802.15.4 to retrieve information from sensors in an agricultural setting. However, the authors concentrate on the size, weight, and power requirements of an UAV. To the best of our knowledge, there are not any previous works that investigate the performances of IEEE 802.15.4, when used by an UAV to communicate with ground sensors in a smart farming context. A partially overlapping work can be found in [10], but it focuses on near-urban and sub-urban environments that differ from rural ones.

Therefore, along the lines of the preliminary works [11] and [12], this letter attempts to fill such a research gap. Specifically, to characterize the packet loss of IEEE 802.15.4 in rural deployments, we propose a *cross-layer* framework using a two-ray path loss (TRPL) model at the physical layer and a Gilbert-Elliott Markov chain to derive the packet loss experienced at the MAC layer. We conducted a very extensive measurement campaign in rural environments, in order to evaluate the effectiveness of the proposed approach. To sum up, the main contributions of this letter are: a refinement of generic models used for IEEE 802.15.4-based applications and an example on how a grid deployment of ground sensors impacts on the packet delivery rate experienced by a mobile UAV, which acts as a data mule.

The rest of this letter is organized as follows. Section II introduces the channel model. Section III discusses the testbed and the obtained measurements, while Section IV provides the characterization of the IEEE 802.15.4 link. Section V concludes the letter.

II. Channel Model

In general, the signal path loss (PL) at 2.4 GHz between two endpoints acting in open space, like a rural field, can be modeled by explicitly taking into account the line of sight component and the reflected one due to the ground effect [13]. The TRPL model allows to calculate the PL, defined as:

$$PL = 10\log_{10}\left(\frac{4\pi d}{\lambda}\right)^2 - 20\log_{10}\left[2\sin\left(\frac{2\pi h_t h_r}{\lambda d}\right)\right], \quad (1)$$

where λ is the wavelength of the considered radio signal, h_t and h_r are the heights of the transmitting and receiving antennas, respectively, and d is the distance between the transmitter and the receiver. All the considered values are in meters. Equation (1) can be used to compute the received signal strength (RSS) in dBm, which is defined as:

$$RSS = P_T + G_t + G_r - PL, \quad (2)$$

where P_T is the transmitted power in dBm, G_t and G_r the transmitting and receiving antenna gains in dBi, respectively.

Equation (2) allows evaluating whether the received information can be successfully decoded or not. To this aim,

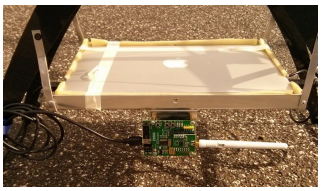

(a) The transmission module deployed on the UAV.

(b) The drone in use in our testbed.

Fig. 1: The IEEE 802.15.4 mobile endpoint implemented on the UAV and the vehicle used in our testbed.

the minimum receiver sensitivity (MRS) in dBm defines the threshold above which the receiver can correctly decode the received data, i.e., when $RSS \geq MRS$. Otherwise, the information is lost.

According to the movements of the UAV, two states can be identified for the link: *i*) a bad state B with $RSS < MRS$ on the average that leads to a packet error rate P_B; *ii*) a good state G with $RSS \geq MRS$ on the average that provides a packet error rate P_G. Let π_G and π_B be the stationary probabilities of being in G and B, respectively. A general approach exploits the Gilbert-Elliott model (see [14], [15]), which is governed by a discrete Markov chain using the information given by RSS to define the behavior of the link with a per-packet granularity. For the sake of completeness, we point out that, if $P_G = 0$, the Gilbert-Elliott model reduces to the Gilbert model. An ON-OFF model refers to the condition $P_B = 1$ and $P_G = 0$. Furthermore, P_G, P_B, π_G, and π_B can be used to compute the average packet loss probability P_{loss}, as defined in [14]:

$$P_{loss} = \pi_G P_G + \pi_B P_B. \tag{3}$$

To recap, the Gilbert-Elliott model can be used to evaluate the performance of a link in terms of packet error rate, while considering two states both characterized by an error probability, as in this work. We point out that, in our testbed, being in the state G (or B) was mainly influenced by the distance d between the IEEE 802.15.4 transceiver on the UAV and the one on the ground. In fact, other impacting parameters, such as h_t, and h_r, are here assumed as constant because they have an almost negligible influence, if compared with the distance.

III. Testbed and Measurements

In this section, we introduce the testbed and the methodology used for the measurement campaign, then we analyze the collected dataset.

A. Testbed and Methodology

To evaluate the performances of the IEEE 802.15.4 link, we performed several tests in a rural field close to Pisa, Italy. Specifically, we considered a line of sight scenario, which perfectly captures many rural-agricultural settings [9], [11], [12]. As extensively done for similar investigations (for instance, see [16] and the references therein), the IEEE 802.15.4 stack has been implemented by using the Waveshare Open2530 board relying on the TI CC253x radio module operating in the 2.4 GHz non-licensed ISM band. Network endpoints have been implemented by using two boards connected to laptops collecting a variety of diagnostic information and usage statistics. According to the standard, a maximum gross rate of 250 kbit/s is expected, along with a transmission range of approximately 150 m. Figure 1a depicts a detail of the payload of the flying vehicle, while Figure 1b showcases the UAV. The UAV in use is an octocopter of about 5 kg, equipped with brushless engines and able to fly at a maximum speed of 130 km/h for about 15-20 minutes, depending on the payload (up to 2.5 kg). If the UAV autonomously follows a path planned offline, the maximum speed is limited to 40 km/h. In this case, the Doppler effect can be neglected [17].

Concerning the methodology used to collect data, the UAV encircled a given area, by automatically tracking some predefined GPS waypoints, as to mimic the inspection of a zone for evaluating the vegetation index or the humidity of the soil. To collect a consistent dataset, repeated flights have been performed at an average flying quota of $h_t = 3$ m. The distance d between the ground transceiver, placed at $h_r = 3.9$ m and the UAV was continuously logged[1]. The values for h_t and h_r were chosen as to have the minimum heights avoiding any obstacles in the flying area. A sensitivity analysis on the heights is out of the scope of this work based on a real testbed.

To have a good tradeoff between the accuracy of the GPS and feasible communication ranges, we considered distances in the $10 - 50$ m range, which can be found in a variety of smart farming applications, including variable rate treatments in precision agriculture [11], [12]. In our testbed, the ground transceiver acts as a IEEE 802.15.4 PAN coordinator.

To guarantee statistical reliability, we conducted more than 20 repeated trials. The two transceivers exchange data by using packets of 50 bits at a rate of $\sim$4 kbit/s. For each packet, we logged the sequence number and a received flag, i.e., a boolean value set to 1 if the packet has been received, or 0 if lost. The quality of the wireless link is evaluated by collecting RSS samples, which are computed by the Open 2530 module by averaging the power received over a eight symbol timeframe. Timestamps are used for synchronizing and correlating data with GPS measurements during the offline processing. The latitude, longitude, and speed of the UAV are provided by the on-board LEA-6 GPS chipset. For all variables, the tracking interval has been set to 0.5 s, as to have a proper tradeoff among accuracy and size of the dataset. The used transmission power P_t is 4.5 dBm, which is the maximum allowed value. For both the receiving and transmitting antennas, the gains G_t and G_r are set to 2 dBi. As it will be shown in Section IV, we did not consider lower values for P_t as this would severely hamper the throughput. The MRS of the IEEE 802.15.4 radio in use is -107 dBm, as reported in the datasheet of the TI CC2530F256 module.

B. Analysis of the Dataset

The dataset collected during the flights is composed of more than 80,000 samples. Figure 2 showcases a partial snapshot.

[1]The ground antenna has been placed on top of a pole to enhance line of sight properties, while sensors and actuators can remain at the ground level near the soil or the vegetation.

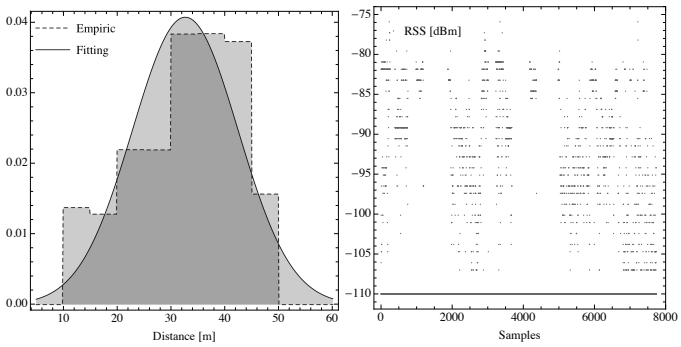

(a) Empiric PDF and best fit. (b) 8,000 samples for the RSS.

Fig. 2: Relevant values of the dataset collected in the measurement campaign.

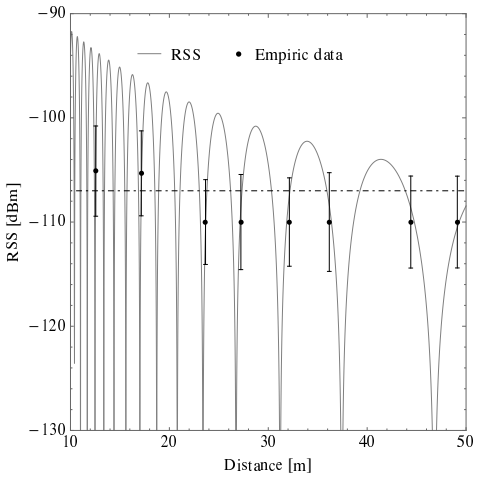

Fig. 3: Different values of RSS in our testbed: the solid grey line is the plot of the model in Equation (2), while black points are measurements. The dashed line is the decoding threshold.

In more detail, Figure 2a depicts the empiric distribution of d during all the flights and the best fitting obtained through a normal distribution with mean 32.6, variance 9.80, and standard deviation 3.13. Figure 2b portraits a subset of 8,000 RSS samples, which has been taken from the whole dataset to estimate the empirical mean. The average condition that $RSS < MRS$ leads to an empirical packet loss rate equal to $\tilde{P}_{loss} = 0.308$.

Figure 3 depicts in black the median values (along with the standard deviation) of the empirical RSS obtained from measurements. The solid grey line represents the model in Equation (2). The horizontal dashed line is the MRS threshold, under which packets cannot be correctly decoded, i.e., $MRS = -107$ dBm. Deviations from median values have been already investigated in [12] and mostly depend on the variability of the flight altitude. In fact, external disturbances, such as the wind or fluctuations in the rotation speed of propellers, may temporarily vary the flight altitude or the alignment of antennas, thus causing misalignment losses. Despite this, the proposed framework applied to our dataset provides a very good fit with the resulting model in Equation (2).

IV. Packet-Level Channel Characterization

In this section, we characterize the link performance at the packet level, especially in terms of packet loss rate. To this aim, we identify a spatial threshold that defines if a packet has been correctly delivered when the channel is in the G or in the B state. According to our investigations, the distance d is the main trigger for a state transition, whereas the effect of other variables is very limited.

Let us denote with D the distribution of the distance d and with $\bar{d}$ the threshold distance that causes a change in the behavior of the link, i.e., the switching from state B to G and vice versa. The conditional error probability when in state G can be calculated as:

$$P_G(\bar{d}) = \int_0^{\bar{d}} RSS(x)D(x)\,dx. \tag{4}$$

Similarly, π_G can be obtained by calculating the probability that $d \leq \bar{d}$:

$$\pi_G(\bar{d}) = \int_0^{\bar{d}} D(x)\,dx. \tag{5}$$

The values in the B state, i.e., P_B and π_B, can be obtained with analogous calculations, by considering $\bar{d} < d \leq 50$ m, the maximum useful distance in our setup. Therefore, combining Equations (3), (4), and (5), the packet loss rate is as follows:

$$P_{loss}(\bar{d}) = \pi_G(\bar{d})P_G(\bar{d}) + \pi_B(\bar{d})P_B(\bar{d}). \tag{6}$$

The distance $\bar{d}^*$, for which Equation (6) approximates Equation (3), can be computed via the following minimization:

$$\bar{d}^* = \underset{\bar{d}}{\operatorname{argmin}} \, ||P_{loss}(\bar{d}) - \tilde{P}_{loss}||^2,$$
$$0 \leq \bar{d} \leq 50. \tag{7}$$

To perform the minimization in (7), we consider for D a normal distribution (see Figure 2a). We obtained $P_{loss}(\bar{d}^*) = 0.304$, which closely matches the empirical packet loss $\tilde{P}_{loss} = 0.308$ computed in Section III-B.

A. Example Application

In the following, we showcase how the model can be used to design the deployment of ground devices interacting with an UAV in agricultural applications and smart farming scenarios. To this aim, we compute $P_G(\bar{d}^*)$, $P_B(\bar{d}^*)$, $\pi_G(\bar{d}^*)$, $\pi_B(\bar{d}^*)$, and the corresponding $P_{loss}(\bar{d}^*)$, by assuming a different distribution D of the distance d. For example, let us consider a grid of sensors deployed on a rural field with varying densities, i.e., a distance of S m between ground nodes arranged on a regular grid. We impose a minimum distance between the UAV and a ground transceiver of at least at $M = 5$ m to minimize the probability of having a collision. Therefore, we drawn d from an uniform distribution D in the range $\left[M, \frac{S}{2}\right]$.

Table I showcases the numerical results computed by using Equations (4), (5), and (6) for different uniform distributions, and providing decreasing coverages. This allows to evaluate the impact of different densities of ground transceivers in terms of packet loss rate, i.e., it provides how many transceivers should be deployed to achieve an average packet loss rate below a desired threshold. For instance, a dense grid would

TABLE I: Probabilities describing the Gilbert-Elliott model.

D	P_G	P_B	π_G	π_B	P_{loss}
$[5, 15]$	0.084	0	1.000	0.000	0.084
$[5, 25]$	0.124	0.193	0.750	0.250	0.141
$[5, 35]$	0.124	0.236	0.500	0.500	0.180
$[5, 45]$	0.124	0.365	0.375	0.625	0.275
$[5, 55]$	0.124	0.443	0.300	0.700	0.347

require deploying a large number of antennas, thus leading to high operational and maintenance costs. Conversely, more sparse deployments could reduce both consumptions and costs, but at the price of higher cross-interferences, or limited possibility of frequency reuse. As an example, referring to Table I, if $S/2 \leq 15$ m, $\pi_B = 0$ and $P_B = 0$, thus resulting in a low P_{loss}. If more distance among the transceivers is expected, e.g., between 15 and 25 m, then an higher P_{loss} should be taken into account. Agricultural applications, which require UAVs with a larger transmission range, should consider that IEEE 802.15.4 links exhibit a not negligible error probability, when the link operates in the state G ($P_{loss} \geq 8\%$, as shown in Table I). This may impose either the use of error recovery techniques, power allocation schemes, or the exploitation of an optimal trajectory [18], as well as hybrid solutions including switching to a different radio link technology. In fact, moving from precision agriculture or smart farming scenarios to different ones (e.g., surveillance), short-range radio systems might be abandoned in favor of long-range technologies, which are characterized by a different tradeoff between the transmission rate, energy consumption, and coverage range.

V. Conclusion and Future Works

In this letter, we discussed the use of IEEE 802.15.4 in smart farming and precision agriculture applications characterized by mobile UAVs communicating with ground sensors. Results indicate that a Gilbert-Elliott model can be suitable to approximate the packet loss rate of the link when the UAV moves in a rural area at low speeds. Since the distance between the communicating endpoints plays a major role, this can be a limit for the use of the IEEE 802.15.4 standard: in fact, the feasible transmission range in our testbed is reduced to approximately 1/3 with respect to the nominal value. When moving to very large rural fields or frameworks requiring beyond-line-of-sight properties, other communication mechanisms may be of interest, as for instance the emerging LoRa / SigFox standards.

Future works aim at refining the model by also considering the impact of different quotas, as well as to understand whether the proposed approach can be used to model the behavior of IEEE 802.15.4 in more general scenarios, e.g., those mixing IoT and industrial applications along with autonomous vehicles.

Acknowledgements

We would like to thank the anonymous reviewers for their thorough review work and the several suggestions provided to improve the quality of this work.

References

[1] L. Gupta, R. Jain, and G. Vaszkun, "Survey of important issues in UAV communication networks," *IEEE Communications Surveys & Tutorials*, vol. 18, no. 2, pp. 1123–1152, 2016.

[2] C. Zhang and J. M. Kovacs, "The application of small unmanned aerial systems for precision agriculture: a review," *Precision agriculture*, vol. 13, no. 6, pp. 693–712, 2012.

[3] M. Mozaffari, W. Saad, M. Bennis, and M. Debbah, "Mobile unmanned aerial vehicles (UAVs) for energy-efficient internet of things communications," *IEEE Transactions on Wireless Communications*, vol. 16, no. 11, pp. 7574–7589, 2017.

[4] T. Rault, A. Bouabdallah, and Y. Challal, "Energy efficiency in wireless sensor networks: A top-down survey," *Computer Networks*, vol. 67, pp. 104–122, 2014.

[5] X. Lin, V. Yajnanarayana, S. D. Muruganathan, S. Gao, H. Asplund, H.-L. Maattanen, M. Bergstrom, S. Euler, and Y.-P. E. Wang, "The sky is not the limit: LTE for unmanned aerial vehicles," *IEEE Communications Magazine*, vol. 56, no. 4, pp. 204–210, 2018.

[6] B. Xia, Q. Fu, D. Li, and L. Zhang, "Performance evaluation and channel modeling of IEEE 802.15.4c in urban scenarios," in *Communications (APCC), 2010 16th Asia-Pacific Conference on*. IEEE, 2010, pp. 497–502.

[7] N. Goddemeier, K. Daniel, and C. Wietfeld, "Coverage evaluation of wireless networks for unmanned aerial systems," in *GLOBECOM, Miami, FL, USA*. IEEE, 2010, pp. 1760–1765.

[8] W. Xiong, X. Hu, and T. Jiang, "Measurement and characterization of link quality for IEEE 802.15.4-compliant wireless sensor networks in vehicular communications," *IEEE Transactions on Industrial Informatics*, vol. 12, no. 5, pp. 1702–1713, 2016.

[9] J. Polo, G. Hornero, C. Duijneveld, A. García, and O. Casas, "Design of a low-cost wireless sensor network with UAV mobile node for agricultural applications," *Computers and electronics in agriculture*, vol. 119, pp. 19–32, 2015.

[10] D. W. Matolak and R. Sun, "Air-Ground Channel Characterization for Unmanned Aircraft Systems - Part III: The Suburban and Near-Urban Environments," *IEEE Transactions on Vehicular Technology*, vol. 66, no. 8, pp. 6607–6618, 2017.

[11] M. Bacco, E. Ferro, and A. Gotta, "UAVs in WSNs for agricultural applications: An analysis of the two-ray radio propagation model," in *SENSORS, 2014 IEEE*. IEEE, 2014, pp. 130–133.

[12] ——, "Radio propagation models for UAVs: What is missing?" in *Proceedings of the 11th International Conference on Mobile and Ubiquitous Systems: Computing, Networking and Services*. ICST (Institute for Computer Sciences, Social-Informatics and Telecommunications Engineering), 2014, pp. 391–392.

[13] P. Barsocchi, G. Oligeri, and F. Potortì, "Measurement-based frame error model for simulating outdoor Wi-Fi networks," *IEEE Transactions on Wireless Communications*, vol. 8, no. 3, pp. 1154–1158, 2009.

[14] N. Celandroni and A. Gotta, "Performance analysis of systematic upper layer FEC codes and interleaving in land mobile satellite channels," *IEEE Transactions on Vehicular Technology*, vol. 60, no. 4, pp. 1887–1894, 2011.

[15] A. Bildea, O. Alphand, F. Rousseau, and A. Duda, "Link quality estimation with the Gilbert-Elliot model for wireless sensor networks," in *Personal, Indoor, and Mobile Radio Communications (PIMRC), 2015 IEEE 26th Annual International Symposium on*. IEEE, 2015, pp. 2049–2054.

[16] L. Tang, K.-C. Wang, Y. Huang, and F. Gu, "Channel characterization and link quality assessment of IEEE 802.15.4-compliant radio for factory environments," *IEEE Transactions on industrial informatics*, vol. 3, no. 2, pp. 99–110, 2007.

[17] J. A. Nazabal, F. Falcone, C. Fernández-Valdivielso, and I. R. Matías, "Development of a low mobility IEEE 802.15.4 compliant VANET system for urban environments," *MDPI Sensors*, vol. 13, no. 6, pp. 7065–7078, 2013.

[18] Q. Wu, Y. Zeng, and R. Zhang, "Joint trajectory and communication design for multi-uav enabled wireless networks," *IEEE Transactions on Wireless Communications*, vol. 17, no. 3, pp. 2109–2121, 2018.